Available online at www.sciencedirect.com
SCIENCE DIRECT®
Thermochimica Acta 407 (2003) 73–84
thermochimica acta
www.elsevier.com/locate/tca

Synthesis and thermal studies on iron(III) complexes of 4-*N*-(4′-antipyrylmethylidene)aminoantipyrine with varying counter ions

N.T. Madhu [a], P.K. Radhakrishnan [b], Matthias Grunert [a], Peter Weinberger [a], Wolfgang Linert [a,*]

[a] *Institute of Applied Synthetic Chemistry, Vienna University of Technology, Getreidemarkt 9/163-AC, A-1060 Vienna, Austria*
[b] *School of Chemical Sciences, Mahatma Gandhi University, Kottayam 686560, Kerala, India*

Received 29 September 2002; received in revised form 25 March 2003; accepted 16 May 2003

Abstract

Iron(III) complexes of the Schiff base 4-*N*-(4′-antipyrylmethylidene)aminoantipyrine (AA) with counter ions, such as, perchlorate, nitrate, thiocyanate, chloride and bromide have been prepared and characterized by elemental analyses, electrical conductance in non-aqueous solvents, IR and electronic spectra, magnetic susceptibility measurements as well as by thermogravimetric analysis. The complexes have the general formulae $[Fe(AA)_2(ClO_4)](ClO_4)_2$, $[Fe(AA)_2X_2]X$ ($X = NO_3^-$ or Br^-) and $[Fe(AA)X_3]$ ($X = SCN^-$ or Cl^-). In complexes, AA acts as a neutral bidentate ligand, coordinating through one of the carbonyl oxygens and azomethine nitrogen in perchlorate, nitrate and bromide complexes while the coordination of AA occurs in a neutral tridentate fashion through both carbonyl oxygens and azomethine nitrogen in thiocyanate and chloride complexes. In the perchlorate complex, one of the perchlorate ions is coordinated bidentately while in the nitrate complex two of the nitrate ions are coordinated monodentately to the metal ion. In the thiocyanate and chloride complexes all the anions are coordinated while in the bromide complex two of the bromide ions are coordinated. A high spin octahedral geometry is assigned to the iron(III) ion in all these complexes. The phenomenological, kinetic and mechanistic aspects of the nitrate, thiocyanate, chloride and bromide complexes were studied by TG and DTG techniques. The kinetic parameters like activation energy, pre-exponential factor and entropy of activation were also computed. The rate controlling process in all stages of decomposition is random nucleation with one on each particle (Mampel model) [Thermochim. Acta 2 (1971) 423].
© 2003 Elsevier B.V. All rights reserved.

Keywords: Iron(III) complexes; Counter ion; 4-*N*-(4′-Antipyrylmethylidene)aminoantipyrine; Fe(III) high spin complexes

1. Introduction

Antipyrine and its derivatives possess antibacterial [1] and antitumor [2] activities. Comparatively little is known on complexes of antipyrine derivatives with 3d-metal ions [3] and their thermal studies. In view of this, and as part of our continuing interest on structural [1,4–6] and thermal [7,8] aspects of antipyrine derivatives, we now report the synthesis and thermal studies of a new series of iron(III) complexes of a Schiff base antipyrine ligand (Fig. 1) with a variety of counter ions such as, perchlorate, nitrate, thiocyanate, chloride and bromide.

* Corresponding author. Tel.: +43-58801-15350; fax: +43-58801-16299.
E-mail address: wlinert@mail.zserv.tuwien.ac.at (W. Linert).

0040-6031/$ – see front matter © 2003 Elsevier B.V. All rights reserved.
doi:10.1016/S0040-6031(03)00309-5

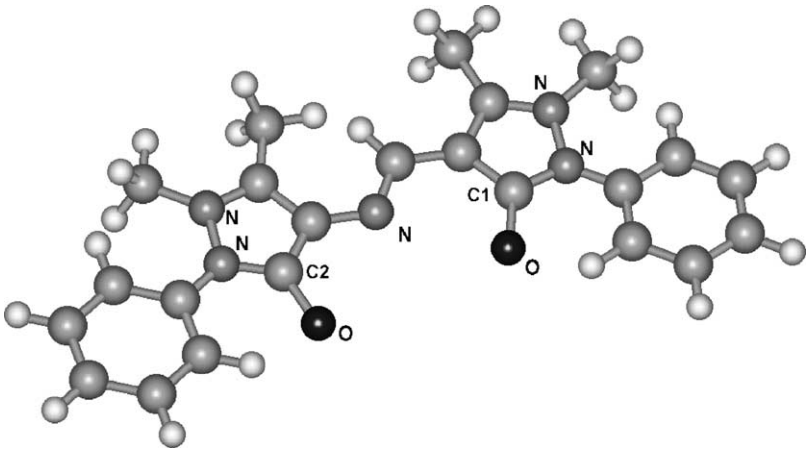

Fig. 1. 4-*N*-(4′-Antipyrylmethylidene)aminoantipyrine.

2. Experimental

2.1. Materials

The metal salts were prepared from Analar ferric carbonate and the respective 50% acids and crystallizing out the salts by evaporating the solution on a steam bath. Ferric thiocyanate was prepared by the method reported earlier [9].

2.2. Preparation of the ligand

The ligand, 4-*N*-(4′-antipyrylmethylidene)aminoantipyrine (AA) was prepared and characterized as previously described [4].

2.3. Preparation of complexes

The metal salt (1 mmol), $Fe(ClO_4)_3{\cdot}6H_2O$, $Fe(NO_3)_3{\cdot}6H_2O$, $Fe(SCN)_3{\cdot}6H_2O$, $FeCl_3{\cdot}6H_2O$ or $FeBr_3{\cdot}6H_2O$ in methanol (10 ml), was added to a boiling solution of 2.2 mmol of AA in acetone (100 ml) for the perchlorate, nitrate and bromide complexes, while 1.2 mmol of AA in methanol (100 ml) for the thiocyanate and chloride complexes. The resulting solution was boiled under reflux for about 2 h on a water bath. For the perchlorate, thiocyanate and chloride complexes, the solid product obtained on refluxing was filtered and washed several times with hot chloroform to remove the excess ligand. It was then recrystallized from acetonitrile.

For the nitrate and bromide complexes, the brown solution so obtained after refluxing was cooled and filtered. On partial evaporation of the solvent and subsequent cooling, the complex was separated which was repeatedly washed with hot benzene to obtain dark brown solid of pure complexes. All the complexes were then dried under vacuum over P_4O_{10}. (Warning: perchlorate salts with organic compounds are potentially explosive. They should be handled in small quantities and with caution.)

2.4. Physical methods of analysis

All the complexes were analyzed for metal and halide content by the standard methods [10] and the perchlorate content by the Kurz method [11]. The electrical conductance of the complexes in acetonitrile, dimethylformamide, methanol and nitrobenzene (10^{-3} M solutions) were measured at room temperature using a Toshniwal conductivity bridge with a dip type conductance cell (cell constant 0.9737, measurement frequency 1591.5 s^{-1}). The infrared spectra of the ligands and the complexes were recorded in the range of 4000–400 cm^{-1} on a Shimadzu IR 470 spectrophotometer and in the range of 400–200 cm^{-1} on a Perkin Elmer 983 IR spectrophotometer. Electronic spectra of the ligands and the complexes in solid state (a paste with nujol) were measured in the range of 200–1100 nm on a Shimadzu UV 160 A spectrophotometer. The elemental analyses (C, H and N) were carried out on a Heraeus CHNO rapid

analyzer. The magnetic moments were measured at room temperature by the Gouy method using mercury(II)tetrathiocyanatocobaltate(II) as the calibrant. Thermogravimetric analyses were undertaken on a Delta Series TGA 7 thermal analyzer in a nitrogen atmosphere (sample mass 10 mg, heating rate at 10 °C/min).

3. Results and discussion

The elemental analyses data (Table 1) suggest that the complexes can be formulated: $Fe(AA)_2X_3$ (X = ClO_4^-, NO_3^- or Br^-) and $Fe(AA)X_3$ (X = SCN^- or Cl^-).

3.1. Electrical conductance

The molar conductance (Table 1) of the perchlorate complex in acetonitrile, dimethylformamide, methanol and nitrobenzene fall in the range expected for 1:2 electrolytes, while for the nitrate and bromide complexes a 1:1 conducting nature [12] is observed. The chloride and thiocyanate complexes behave as non-electrolytes [12]. Thus, these may be formulated as $[Fe(AA)_2(ClO_4)](ClO_4)_2$, $[Fe(AA)_2X_2]X$ (X = NO_3^- or Br^-) and $[Fe(AA)X_3]$ (X = SCN^- or Cl^-).

3.2. IR spectra

The important spectral data of AA and its complexes are presented in Table 2. AA exhibits two strong bands at 1643 and 1659 cm^{-1}, corresponding to the C^1=O and C^2=O stretching vibrations [4], respectively (Fig. 2). The band $\nu(C^1{=}O)$ of AA is shifted to the 1620–1624 cm^{-1} region in the perchlorate, nitrate and bromide complexes indicating coordination of carbonyl oxygen [4] of C^1=O. However, the band corresponding to $\nu(C^2{=}O)$ remains practically unaltered at about 1656 cm^{-1} indicating the non-coordination of carbonyl oxygen [4] of C^2=O. In the thiocyanate and chloride complexes, the $\nu(C^1{=}O)$ and $\nu(C^2{=}O)$ bands are shifted to 1618 and 1628 cm^{-1}, respectively, indicating the coordination of both the carbonyl oxygens [6]. An intense band observed at 1596 cm^{-1} attributable to the C=N stretching vibration [4] in AA is shifted to about 1606 cm^{-1} in all these complexes, indicating the coordination of the azomethine nitrogen [4].

In the perchlorate complex, the triply split band maxima at 1140, 1115 and 1025 cm^{-1} are due to the ν_8, ν_6, and ν_1 vibrations, respectively, of bidentate coordination thereof (C_{2v}) [13,14]. The band at 1085 cm^{-1} is assigned to the ν_3 vibration of the uncoordinated perchlorate [13] ion (T_d). In addition to this, the vibrational frequencies at 940 and 638 cm^{-1} corresponding to the ν_2 and ν_3 vibrations, respectively, of the perchlorate (C_{2v}) ion and the band at 624 cm^{-1} due to the ν_4 vibration of the perchlorate (T_d) ion also support the co-existence of both bidentate coordinated and uncoordinated perchlorate ions in this complex [13,14].

For the nitrate complex, the presence of coordinated nitrate ions are indicated by two medium intensity bands at 1420 and 1315 cm^{-1} due to the ν_4 and ν_1 vibrations, respectively, of the nitrate ion of C_{2v} symmetry [15]. Since $(\nu_4 - \nu_1) = 105\ cm^{-1}$, the nitrate ions are coordinated in a unidentate fashion [15]. Besides a very strong band at 1380 cm^{-1} and a medium intensity band at 825 cm^{-1} are due to the ν_3 and ν_2 vibrations, respectively, of the uncoordinated nitrate ion (D_{3h}) [16].

In the thiocyanate complex, a sharp band at 2050 cm^{-1} is indicative of N coordinated thiocyanate ion [16]. Furthermore, the presence of bands at 850 and 480 cm^{-1} stands as additional evidence for N coordinated thiocyanate ion [16].

In the far IR spectra halide complexes, the Fe–Cl and Fe–Br stretching vibrations occurs [16] at 312 and 282 cm^{-1}, respectively, which are absent in the ligand spectrum.

These spectral observations along with the conductance data indicate that one of the perchlorates, two of the nitrates and bromides, all the thiocyanates and chlorides are coordinated to the metal ion in these complexes. In addition, the ν(Fe–O) and ν(Fe–N) stretching vibrations are at about 550 and 440–450 cm^{-1}, respectively, in complexes [4,5].

3.3. Electronic spectra

The spectra of AA and its complexes with tentative assignments are presented in Table 3. AA shows two band maxima at 28,570 and 40,485 cm^{-1} corresponding to $n \rightarrow \pi^*$ and $\pi \rightarrow \pi^*$ transitions [4],

Table 1
Analytical and conductance data of the obtained complexes

Complex	Formula weight	Weight of the complex formed (g)	Yield (%)	Found (calculated) (%)					Molar conductance (Ω^{-1} cm^2 mol^{-1})			
				Iron	X[a]	C	H	N	$PhNO_2$	MeCN	DMF	MeOH
$[Fe(AA)_2(ClO_4)](ClO_4)_2$	1157.01	0.4223	73.00	4.9 (4.8)	25.7 (25.7)	47.7 (47.7)	3.9 (4.0)	12.1 (12.1)	51.6	262.9	146.0	178.6
$[Fe(AA)_2(NO_3)_2]NO_3$	1044.59	0.3663	70.15	5.4 (5.3)	–	52.7 (52.9)	4.3 (4.4)	17.4 (17.4)	19.2	160.6	89.6	94.5
$[Fe(AA)(SCN)_3]$	631.48	0.4305	68.18	8.9 (8.8)	–	49.3 (49.5)	3.5 (3.6)	17.5 (17.7)	9.8	77.9	63.5	51.2
$[Fe(AA)Cl_3]$	563.60	0.4007	71.10	9.9 (9.9)	18.9 (18.9)	49.0 (49.0)	4.1 (4.1)	12.4 (12.4)	3.8	73.6	40.1	47.6
$[Fe(AA)_2Br_2]Br$	1098.36	0.4389	79.92	5.1 (5.1)	21.9 (21.8)	50.3 (50.3)	4.2 (4.2)	12.8 (12.7)	34.9	130.9	75.1	96.6

[a] $X = ClO_4^-$, Cl^- or Br^-.

Table 2
Important IR spectral bands (cm^{-1}) of the obtained complexes[a]

AA	$[Fe(AA)_2(ClO_4)](ClO_4)_2$	$[Fe(AA)_2(NO_3)_2]NO_3$	$[Fe(AA)(SCN)_3]$	$[Fe(AA)Cl_3]$	$[Fe(AA)_2Br_2]Br$	Assignment
1643 s	1620 s	1623 s	1618 s	1628 s	1624 s	$\nu(C^1{=}O)$
1659 s	1655 s	1656 s	1618 s	1628 s	1656 s	$\nu(C^2{=}O)$
1596 s	1606 s	1606 s	1606 s	1606 s	1606 s	ν(C=N)
–	1140 m	–	–	–	–	ν_8—coordinated ClO_4^-
–	1115 s	–	–	–	–	ν_6—coordinated ClO_4^-
–	1025 m	–	–	–	–	ν_1—coordinated ClO_4^-
–	940 w	–	–	–	–	ν_2—coordinated ClO_4^-
–	638 w	–	–	–	–	ν_3—coordinated ClO_4^-
–	1085 s	–	–	–	–	ν_3—ionic ClO_4^-
–	624 m	–	–	–	–	ν_4—ionic ClO_4^-
–	–	1420 m	–	–	–	ν_4—coordinated NO_3^-
–	–	1315 m	–	–	–	ν_1—coordinated NO_3^-
–	–	1380 s	–	–	–	ν_3—ionic NO_3^-
–	–	825 m	–	–	–	ν_2—ionic NO_3^-
–	–	–	2050 s	–	–	ν(C–N)
–	–	–	850 w	–	–	ν(C–S)
–	–	–	480 m	–	–	δ(NCS)
–	–	–	–	312 m	–	ν(Fe–Cl)
–	–	–	–	–	282 m	ν(Fe–Br)
–	550 w	555 w	550 w	550 w	550 w	ν(Fe–O)
–	445 w	450 w	440 w	450 w	440 w	ν(Fe–N)

[a] s: strong; m: medium; w: weak.

respectively. In complexes, both n → π* and π → π* bands are found as blue shifted and appeared in the region 28,735–29,761 and 42,016–45,871 cm^{-1} regions, respectively, compared to that of AA. All the complexes exhibit a band in the 19,417–21,596 cm^{-1} range corresponding to the $^6A_{1g} \rightarrow {}^4T_{1g}$ transition consistent with octahedral Fe(III) complexes [17,18]. Furthermore, a strong band at 32,258 cm^{-1} in complexes corresponds to charge transfer transition [4].

3.4. Magnetic moment data

The molar magnetic moments of the complexes are presented in Table 3. The values are in the 5.84–6.00 BM range, suggesting a high spin octahedral geometry around Fe(III) ion [19,20].

Based on the results of this study, the structures shown in Fig. 2 may be assigned to the complexes.

3.5. Phenomenological aspects

The TG and DTG curves of the complexes are given in Figs. 3–6 and the corresponding thermal analysis data is presented in Table 4.

For the perchlorate complex, there is no mass loss up to 205 °C indicating that either water or solvent molecules are absent in this complex. Above 205 °C, the thermal studies could not be conducted due its explosive nature.

In the case of nitrate complex (Fig. 3), the decomposition occurs in the 157–496 °C range. There is no mass loss up to 157 °C revealing the absence of either water or solvent molecules in this complex. The first stage of decomposition starts at 157 °C and ends at 241 °C. The observed mass loss (17.14%) is due to the decomposition of three nitrate ions and which is in agreement with a calculated mass loss of 17.79%. This result is supported by the absence of nitrate ion in the intermediate compound obtained at 241 °C as confirmed by IR spectral analysis. The maximum rate of mass loss occurs at 231 °C as indicated by the DTG peak. The second stage starts at 241 °C and ends at 420 °C with the DTG peak at 348 °C. The corresponding mass loss (37.14%) is attributed to the decomposition of one ligand molecule. The third stage starts at 420 °C and comes to an end at 496 °C with DTG peak at 473 °C and the corresponding mass loss (37.91%) is due to the decomposition of the remaining ligand

molecule. The mass losses in the second and third stages are in agreement with a calculated mass loss of 38.42%. The decomposition completes at 496 °C and the final residue is qualitatively proved to be anhydrous metal oxide.

For the thiocyanate complex (Fig. 4), there is no mass loss up to 218 °C indicating that either water or solvent molecules are absent in this complex. It undergoes a two-stage decomposition process. The first stage starts at 218 °C and ends at 455 °C with the DTG peak at 321 °C. The corresponding mass loss (39.28%) is attributed to the decomposition of half of the ligand molecule and one thiocyanate ion and which is in agreement with a calculated mass loss of 40.97%. The IR spectrum of the residue after this stage shows the presence of AA and thiocyanate ion indicating only

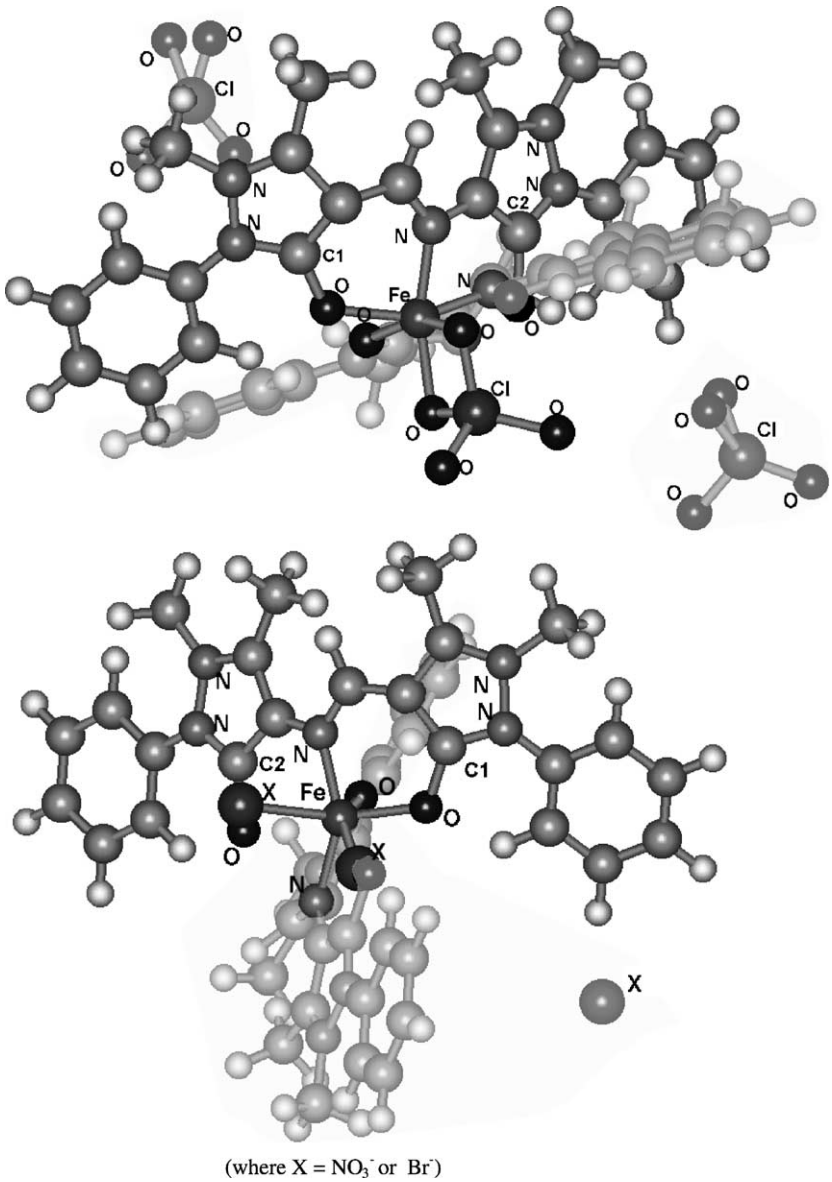

Fig. 2. Tentative structures of Fe(III) complexes of AA with perchlorate, nitrate, thiocyanate, chloride and bromide as counter ions.

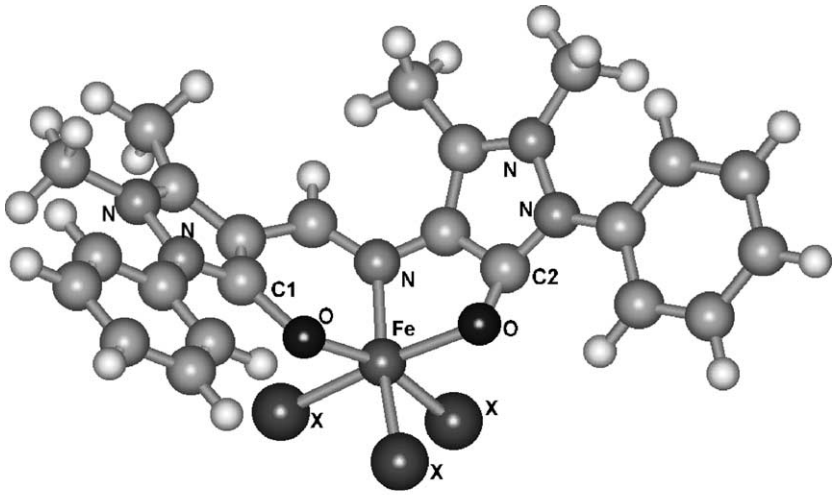

(Where X = SCN^- or Cl^-)

Fig. 2. (*Continued*).

Table 3
Electronic spectral data and magnetic moments of the obtained complexes

Complex	Band. max. (cm^{-1})	Tentative assignments	μ_{eff} (BM)
AA	28570	$n \rightarrow \pi^*$	–
	40485	$\pi \rightarrow \pi^*$	
$[Fe(AA)_2(ClO_4)](ClO_4)_2$	28735	$n \rightarrow \pi^*$	5.85
	42372	$\pi \rightarrow \pi^*$	
	32258	Charge transfer	
	19417	$^6A_{1g} \rightarrow {}^4T_{1g}$	
$[Fe(AA)_2(NO_3)_2]NO_3$	29761	$n \rightarrow \pi^*$	5.92
	43478	$\pi \rightarrow \pi^*$	
	32258	Charge transfer	
	19723	$^6A_{1g} \rightarrow {}^4T_{1g}$	
$[Fe(AA)(SCN)_3]$	28901	$n \rightarrow \pi^*$	5.94
	42735	$\pi \rightarrow \pi^*$	
	32258	Charge transfer	
	21276	$^6A_{1g} \rightarrow {}^4T_{1g}$	
$[Fe(AA)Cl_3]$	28985	$n \rightarrow \pi^*$	5.95
	42016	$\pi \rightarrow \pi^*$	
	32258	Charge transfer	
	20618	$^6A_{1g} \rightarrow {}^4T_{1g}$	
$[Fe(AA)_2Br_2]Br$	28818	$n \rightarrow \pi^*$	6.00
	45871	$\pi \rightarrow \pi^*$	
	32258	Charge transfer	
	21596	$^6A_{1g} \rightarrow {}^4T_{1g}$	

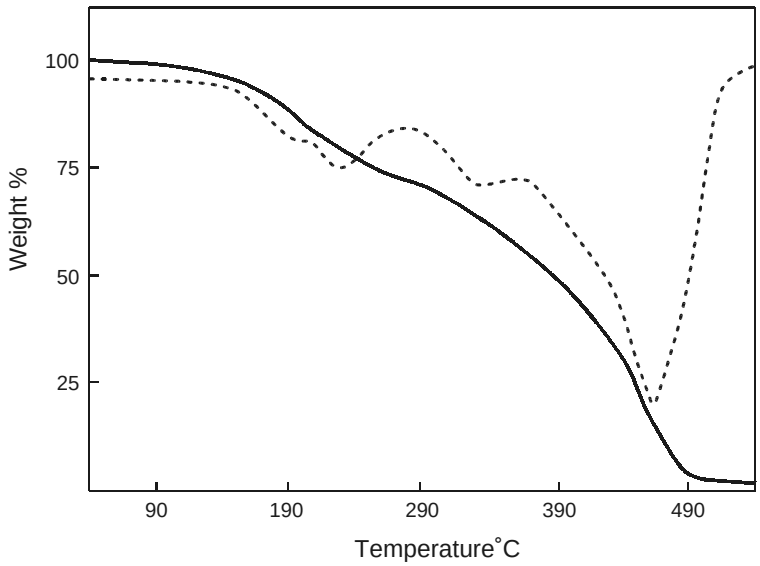

Fig. 3. TG and DTG curves of $[Fe(AA)_2(NO_3)_2]NO_3$ (nitrogen at a heating rate of 10 °C/min; —: TG; - - -: DTG).

partial removal of AA and thiocyanate at this stage. The second stage starts at 455 °C and comes to an end at 564 °C with the DTG peak at 529 °C. The corresponding mass loss (50.70%) is due to the decomposition of the remaining half of the ligand molecule and two thiocyanate ions and which is in agreement with a calculated mass loss of 50.17%. The decomposition of the complex completes at 564 °C and the final residue is qualitatively proved to be anhydrous metal oxide.

For the chloride complex (Fig. 5), there is no mass loss up to 260 °C indicating that either water or solvent molecules are absent in this complex. It undergoes a

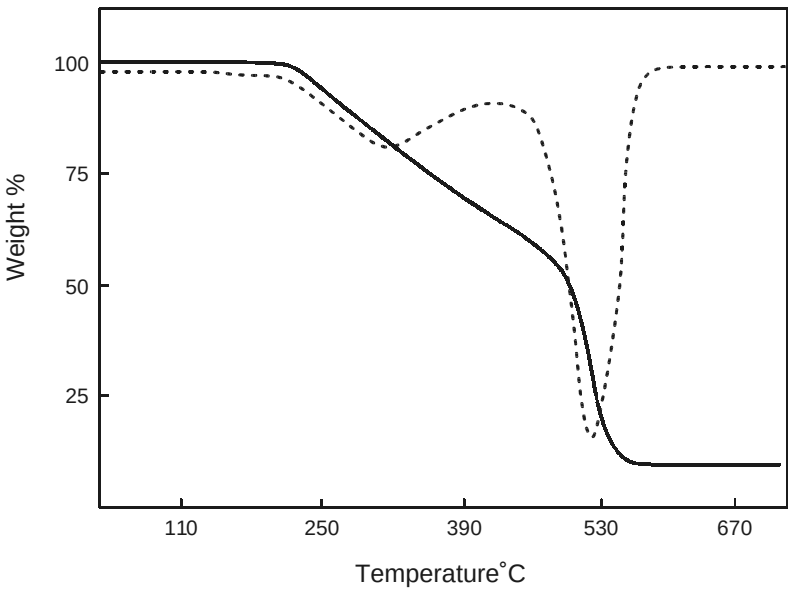

Fig. 4. TG and DTG curves of $[Fe(AA)(SCN)_3]$ (in nitrogen at a heating rate of 10 °C/min; —: TG; - - -: DTG).

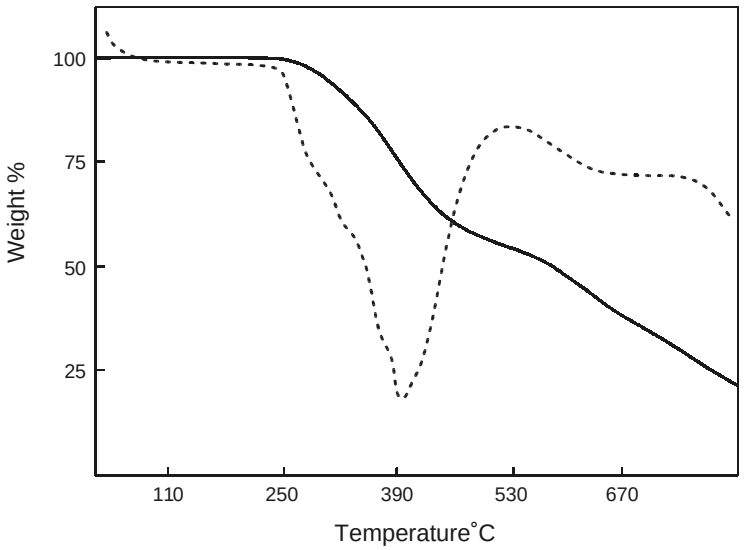

Fig. 5. TG and DTG curves of $[Fe(AA)Cl_2]$ (in nitrogen at a heating rate of 10 °C/min; —: TG; - - -: DTG).

two-stage decomposition process. The first stage starts at 260 °C and ends at 573 °C with the DTG peak at 398 °C. The corresponding mass loss (34.49%) is attributed to the decomposition of half of the molecule of AA and which is in agreement with a calculated mass loss of 35.61%. The IR spectrum of the residue after this stage shows the presence of AA indicating only partial removal of the ligand at this stage. The second stage of decomposition, which starts at 573 °C, is a continuous one. The steady mass loss observed

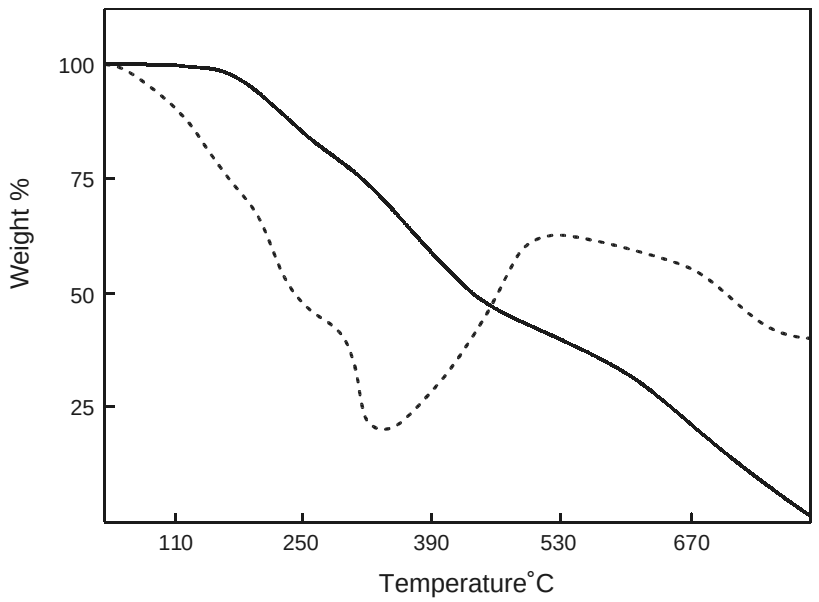

Fig. 6. TG and DTG curves of $[Fe(AA)_2Br_2]Br$ (in nitrogen at a heating rate of 10 °C/min; —: TG; - - -: DTG).

Table 4
Phenomenological data for the thermal decomposition of the obtained complexes

Complex	Stage of decomposition	TG plateau (°C)	DTG peak (°C)	Found (calculated) (%)
$[Fe(AA)_2(NO_3)_2]NO_3$	I	157–241	231	17.14 (17.79)
	II	241–420	348	37.14 (38.42)
	III	420–496	473	37.91 (38.42)
$[Fe(AA)(SCN)_3]$	I	218–455	321	39.28 (40.97)
	II	455–564	529	50.70 (50.17)
$[Fe(AA)Cl_3]$	I	260–573	398	34.49 (35.61)
	II	573	–	Continuous
$[Fe(AA)_2Br_2]Br$	I	171–426	335	36.54 (36.54)
	II	426	–	Continuous

in this stage may be due to the expulsion of the remaining part of the ligand molecule together with the volatilization of the residue of anhydrous metal chloride [21].

The bromide complex (Fig. 6), undergoes a two-stage decomposition process and there is no mass loss up to 171 °C revealing the absence of either water or solvent molecules in this complex. The first stage of decomposition starts at 171 °C and ends at 426 °C with the DTG peak at 335 °C. The corresponding mass loss (36.54%) is due to the decomposition of one molecule of AA and which in agreement with a calculated mass loss of 36.54%. The second stage, which begins at 426 °C, is a continuous one. The steady mass loss observed in this stage may be due to the expulsion of the remaining ligand molecule together with the volatilization of the residue of anhydrous metal bromide [21].

3.6. Kinetic aspects

All the well characterized decomposition stages of the nitrate, thiocyanate, chloride and bromide complexes were selected for the study of the kinetics of decomposition. The kinetic parameters like the activation energy (E) and the pre-exponential factor (A) were calculated for all the well defined stages of decomposition using Coats–Redfern equation [22]:

$$\log\left[\frac{g(\alpha)}{T^2}\right] = \log\frac{AR}{\phi E}\left[1 - \frac{2RT}{E}\right] - \frac{E}{2.303RT}$$

where T is the temperature, A the pre-exponential factor, R the gas constant, φ the heating rate and E the activation energy.

In the present investigation $\log[g(\alpha)/T^2]$ plotted against $10^3/T$ gives straight lines whose slope and intercept are used to evaluate the kinetic parameters by the least squares method. The goodness of fit is checked by calculating the correlation coefficient.

The entropy of activation (ΔS) is also calculated for each stage of thermal decomposition in these complexes using the relationship:

$$A = \frac{kT_s}{h}\, e^{\Delta S/R}$$

where A is the pre-exponential factor, k the Boltzmann constant, T_s the peak temperature, ΔS the entropy of activation and R the gas constant. All the calculations were done with the help of a computer program.

The values of various kinetic parameters calculated are given in Table 5. The activation energies (E) in the different stages of thermal decomposition of iron(III) complexes are in the range of 28.25–249.95 kJ mol^{-1}. The corresponding values of pre-exponential factor (A) are in the range of 2.40×10^{-2}–1.16×10^5 s^{-1}. The respective values of the entropy of activation (ΔS) are in the range of -281.81 to -153.02 J mol^{-1} range. Neither the values of A nor the values ΔS show a definite trend along the series, but the energy of activation for the second-stage decomposition of nitrate and thiocyanate complexes is higher than that of the first stage. This may be due to the less steric strain in the intermediate compound obtained after the first stage.

On comparing the activation energies of the second stage of decomposition of the nitrate and thiocyanate complex, the latter show remarkably higher value. This may also be due to the less steric strain for the intermediate compound formed for the thiocyanate complex

Table 5
Kinetic parameters for the thermal decomposition of the obtained complexes

Complex	Stage	E (kJ mol^{-1})	A (s^{-1})	ΔS (J K mol^{-1})
$[Fe(AA)_2(NO_3)_2]NO_3$	I	47.65	0.59	−253.61
	II	48.67	0.17	−265.35
	III	225.48	1.16×10^5	−155.53
$[Fe(AA)(SCN)_3]$	I	36.74	5.56×10^{-2}	−274.65
	II	249.95	1.69×10^5	−153.02
$[Fe(AA)Cl_3]$	I	50.82	0.15	−267.19
$[Fe(AA)_2Br_2]Br$	I	28.25	2.40×10^{-2}	−281.81

Table 6
Correlation coefficients calculated using the nine forms of $g(\alpha)$ for the obtained complexes

No.	Form of $g(\alpha)$	Correlation coefficient (r)						
		Nitrate complex			Thiocyanate complex		Chloride complex, stage I	Bromide complex, stage I
		Stage I	Stage II	Stage III	Stage I	Stage II		
1	α^2	−0.9875	−0.9939	−0.9783	−0.9883	−0.9883	−0.9464	−0.9893
2	$\alpha + (1-\alpha)\ln(1-\alpha)$	−0.9936	−0.9986	−0.9887	−0.9947	−0.9940	−0.9684	−0.9949
3	$[1-(1-\alpha)^{1/3}]^2$	−0.9764	−0.9942	−0.9739	−0.9657	−0.9862	−0.8715	−0.9606
4	$[1-(2/3)\alpha]-(1-\alpha)^{2/3}$	−0.9956	−0.9990	−0.9926	−0.9966	−0.9958	−0.9776	−0.9966
5	$-\ln(1-\alpha)$	−0.9996	−0.9999	−0.9992	−0.9993	−0.9997	−0.9992	−0.9994
6	$[-\ln(1-\alpha)]^{1/2}$	−0.9993	−0.9998	−0.9991	−0.9987	−0.9996	−0.9980	−0.9982
7	$[-\ln(1-\alpha)]^{1/3}$	−0.9991	−0.9988	−0.9989	−0.9961	−0.9995	−0.9938	−0.9911
8	$1-(1-\alpha)^{1/2}$	−0.9955	−0.9989	−0.9939	−0.9959	−0.9963	−0.9748	−0.9953
9	$1-(1-\alpha)^{1/3}$	−0.9976	−0.9994	−0.9973	−0.9981	−0.9981	−0.9868	−0.9976

compared to that of nitrate complex. But, the negative values of entropy of activation indicate that the activated complex has a more ordered structure than the reactants [7,8].

3.7. Mechanistic aspects

The assignment of the mechanism of thermal decomposition is based on the assumption that the form of $g(\alpha)$ depends on the reaction mechanism. In the present investigation, nine forms of $g(\alpha)$, suggested by Satava [23], are used to enunciate the mechanism of thermal decomposition in each stage. The correlation coefficient for all these nine forms were calculated and the form of $g(\alpha)$ for which the correlation has a maximum value is chosen as the mechanism of reaction (Table 6). We have calculated the kinetic parameters of the thermal decomposition of iron(III) nitrate, thiocyanate, chloride and bromide of AA using all the well defined decomposition stages. In the present investigation, the highest value of correlation coefficient is obtained for

$$g(\alpha) = -\ln(1-\alpha)$$

in all stages of decomposition of the present complexes. Hence the mechanism of decomposition is the random nucleation with one nucleus on each particle. This represents the 'Mampel model' [7,8,23].

4. Conclusion

Iron(III) complexes of the Schiff base ligand AA, have been synthesized and characterized by various physicochemical studies and an octahedral geometry is assigned to all the complexes.

The TG results show that though the stoichiometry of the nitrate and bromide complexes is the same, the bromide complex is more stable than the nitrate complex. The nitrate complex undergoes a three-stage

decomposition while the bromide complex decomposes in two stages. The thiocyanate and chloride complex, the molecular compositions of which are different from that of nitrate and bromide complexes follow a two-stage decomposition pattern and undergo decomposition at higher temperatures compared to that of nitrate and bromide complexes. The chloride complex decomposes at higher temperature than the thiocyanate complex. The chloride complex is the most stable and the nitrate complex is the least stable among the series.

There is no definite trend observed either in the value of A or in the value of ΔS in the different stages of decomposition among the series. But the activation energy can be correlated to the steric strain occurred for the intermediate compound.

The mechanism for the solid state thermal decomposition for all the complex is found to be random nucleation with one nucleus on each particle. This represents the—Mampel model.

Acknowledgements

Thanks for financial support due to the “Fonds zur Förderung der Wissenschaftlichen Forschung in Österreich” (project 15874-N03), and the European Science Foundation ESF within the project “Molecular magnets” are gratefully acknowledged.

References

[1] M. Alaudeen, A. Abraham, P.K. Radhakrishnan, Proc. Ind. Acad. Sci. (Chem. Sci.) 107 (1995) 57.
[2] C.J. Alice, C.P. Prabhakaran, Trans. Met. Chem. 15 (1990) 449.
[3] A.M. Donia, F.A. El-Saied, Polyhedrdron 21 (1988) 2149.
[4] N.T. Madhu, P.K. Radhakrishnan, Trans. Met. Chem. 25 (2000) 287.
[5] N.T. Madhu, P.K. Radhakrishnan, Synth. React. Inorg. Met.-Org. Chem. 30 (2000) 1561.
[6] N.T. Madhu, P.K. Radhakrishnan, Synth. React. Inorg. Met.-Org. Chem. 31 (2001) 315.
[7] M.K.M. Nair, P.K. Radhakrishnan, J. Therm. Anal. Calorim. 52 (1998) 475.
[8] C.R. Vinodkumar, M.K.M. Nair, P.K. Radhakrishnan, J. Therm. Anal. Calorim. 61 (2000) 143.
[9] A.N.S. Ram, S. Sarasukutty, C.P. Prabhakaran, Curr. Sci. (India) 45 (1976) 514.
[10] A.I. Vogel, A Text Book of Quantitative Inorganic Analysis, ELBS, London, 1961.
[11] E. Kurz, G. Kober, M. Berl, Anal. Chem. 30 (1958) 1983.
[12] W.J. Geary, Coord. Chem. Rev. 7 (1971) 81.
[13] R.P. Scholer, A.E. Merbach, Inorg. Chim. Acta 15 (1975) 15.
[14] B.J. Hathaway, A.E. Underhill, J. Chem. Soc. (1961) 3091.
[15] K. Nakamoto, Infrared and Raman Spectra of Inorganic and Coordination Compounds, Wiley, New York, 1986.
[16] B.M. Gatehouse, S.E. Livingstone, R.S. Nyholm, J. Inorg. Nucl. Chem. 8 (1958) 75.
[17] K.K. Narang, V.P. Singh, Synth. React. Inorg. Met.-Org. Chem. 23 (1993) 971.
[18] A.B.P. Lever, Inorganic Electronic Spectroscopy, 2nd ed., Elsevier, Amsterdam, 1984.
[19] M.S. Islam, M.M. Uddin, Synth. React. Inorg. Met.-Org. Chem. 21 (1991) 1093.
[20] F.A. Cotton, G. Wilkinson, Advanced Inorganic Chemistry, 3rd ed., Wiley, New Delhi, 1992.
[21] J.A. Dean (Ed.), Langes Hand Book of Chemistry, 13th ed., McGraw-Hill, New York, 1976.
[22] A.W. Coats, J.P. Redfern, Nature 201 (1964) 68.
[23] V. Satava, Thermochim. Acta 2 (1971) 423.